Efficient microfluidic particle separation arrays

David W. Inglis

Department of Physics, Macquarie University
Sydney, NSW, 2109, Australia

September 29, 2008

Abstract

Microfluidic particle separation arrays are capable of passive sorting of microparticles or cells by size while avoiding blockage. Separation efficiency is severely degraded in the areas adjacent to the boundaries due to the aberrant fluid flow found there. This letter shows how to eliminate this problem by modifying the boundary interface. At each row the boundary is moved by a specific amount to ensure a linear change in flux from row to row which leads to uniform flow patterns and improved separation characteristics throughout the array.

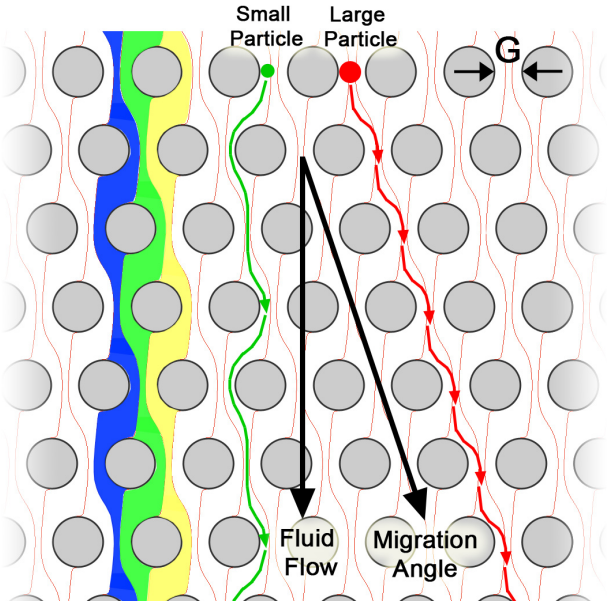

Figure 1: Illustration showing the separation method. The periodic flow patterns, or streamlines, are highlighted in blue, green and yellow, a small particle, green, is able to follow the fluid flow, while the large particle, red, is excluded from the leftmost streamline in each gap. This causes the large particle to move at and angle to the flow fluid and makes separation possible.

Passive separation of microparticles by size can be accomplished in two-dimensional arrays of posts called deterministic lateral displacement (DLD) arrays [1, 2]. These separation devices have high resolution (up to 2% of particle diameter), are inexpensive, simple to operate and capable, for example of separating different cell types in blood [3] and extracting whole bacterial chromosomes [4]. Separation occurs because particles above a critical size, but significantly less than the minimum gap size, move at a migration angle, θ, relative to fluid flow. Figure 1 is an illustration of how the post array, and subsequent flow patterns are able to differentiate large from small particles. Briefly, if a particle is too large to fit within the left-most streamline in a gap it cannot follow the net vertical flow and is instead displaced laterally by a small amount at each row.

Previous work has described the flow patterns responsible for separation and consistently shown predictable results provided the measurements are made in very wide arrays, far from any boundaries or discontinuities that would disturb the flow patterns. However, practical considerations often require the use of boundaries and narrow arrays. The boundaries make it possible to concentrate particles of a particular size, and multiple narrow arrays in parallel have lower fluidic resistance, leading to higher throughput, than comparable single arrays. However the presence of such boundaries disturbs the periodic flow patterns, reducing or

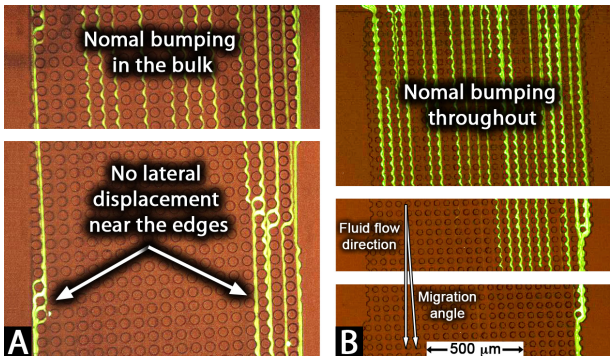

Figure 2: Image collage showing beads that are significantly above (∼50%) the critical particle size in an array with uncorrected (A), and corrected (B) edges. The array in (A) has 19.5-μm gaps, 43-μm posts, and a slope of 1/20, giving a nominal critical size of 6.5 μm. The beads (Polysciences) are 10.0 μm in diameter, 56% above the critical size. In (B) the posts are 25.5 μm, the gap is 17.5 μm, with $\epsilon = 1/20$, giving a critical particle size of 5.8 μm.

eliminating the separation effect. This letter presents a solution to the problem. The solution is developed theoretically, then numerically simulated and verified experimentally.

We consider a device with a single input, designed to concentrate particles, as shown in Figure 2. Particles enter the top of the device and those above the critical size move at an angle θ to the fluid flow. The critical size is a function of the slope or row shift fraction $\epsilon = \tan(\theta)$. Ideally all particles greater than the critical size are concentrated along the right wall after a length given by the array width divided by the tangent of the migration angle θ. Without thoughtful engineering, both the left (depletion) boundary and the right (enrichment) boundary fail to laterally displace particles, as in Figure 2A, leading to poor concentration and residual particles left in the solution.

The separation mechanism relies on a small amount of fluid flux, a streamline, to move left over the top of each post, (see Morton et al. [5] for a more thorough description). The width of this streamline determines the critical particle size. Having a uniform critical size is essential for efficient separation. The amount of fluid flux that moves left over the top of each post in the ideal array is $\Phi\epsilon$ where Φ is the total fluid flux through the gap. The boundary drastically affects this quantity in the nearby posts. Our solution to maintain the value of $\Phi\epsilon$ relies on appropriate control of the first and the last gap in each row. Namely, on the left boundary the width of the gap in the n^{th} row is chosen as

$$g_n = G\sqrt{n\epsilon}, \tag{1}$$

where n goes from 1 to $\frac{1}{\epsilon}$ and G is the nominal gap in the array. This ensures that the n^{th} gap adjacent to the left boundary accepts the fluid from the $(n-1)$ gap immediately

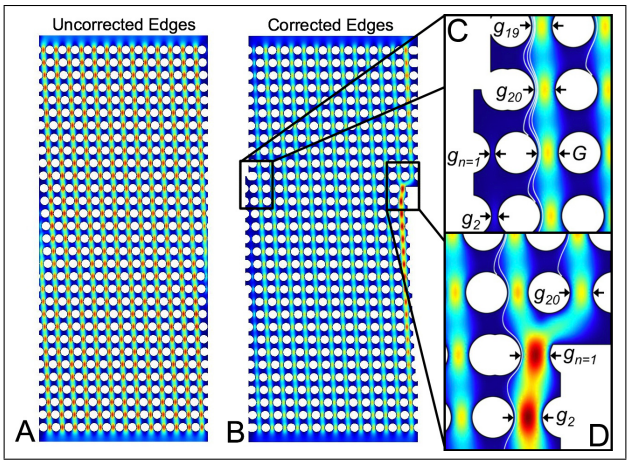

Figure 3: Fluid simulations showing models with uncorrected (A) and corrected (B) edges. A closer look at the left (C) and right (D) edges showing a few stall-lines.

above plus one streamline from the gap immediately above and to the right. On the right boundary the gap in the n-th row is:

$$g_n = G\sqrt{2 - n\epsilon}. \tag{2}$$

This ensures that the n^{th} gap adjacent to the right boundary pushes one streamline into the gap one row down and one row left. The factor of 2 in Equation 2 provides for a wide enough gap to prevent clogging as the particles concentrate against the right boundary. By adjusting the two gaps in each row at the boundaries we maintain a uniform $\Phi\epsilon$ thus simulating the behaviour of an infinite array while retaining the advantages of a finite one.

This approach is first verified by two dimensional fluid simulations. Using COMSOL Multiphysics® (Burlington MA), two similar DLD arrays were compared. Figure 3A has vertical or uncorrected edges, while Figure 3B has edges modulated according to the principles given above. The arrays are 400 μm wide and 970 μm long, and they contain 31 rows and 13 columns. All surfaces are non-slip with flow driven by uniform pressure across the top edge. The gap, G, is 10 μm, the post diameter is 20 μm, and the row shift fraction, ϵ, is 1/20, so after 20 rows the array repeats itself. Figure 3C shows a close up view of the left edge at the onset of the smallest gap, ($g_{n=20} = G = 10$ μm, $g_{n=1} = 2.24$ μm, $g_{n=2} = 3.16$ μm according to Eq. 1).

Along the right (enrichment) edge $g_{n=1} = \sqrt{1.95}G$ is the largest gap as it must collect fluid from two columns (Fig. 3D). The next gap, g_2 is slightly smaller, as is g_3 and so on so that as the fluid progresses down the column the flux in that column decreases, by $\Phi\epsilon$ at each row.

Not only does correcting the edges improve performance near those edges but simulations indicate improved performance in the center of the array. We have compared the two

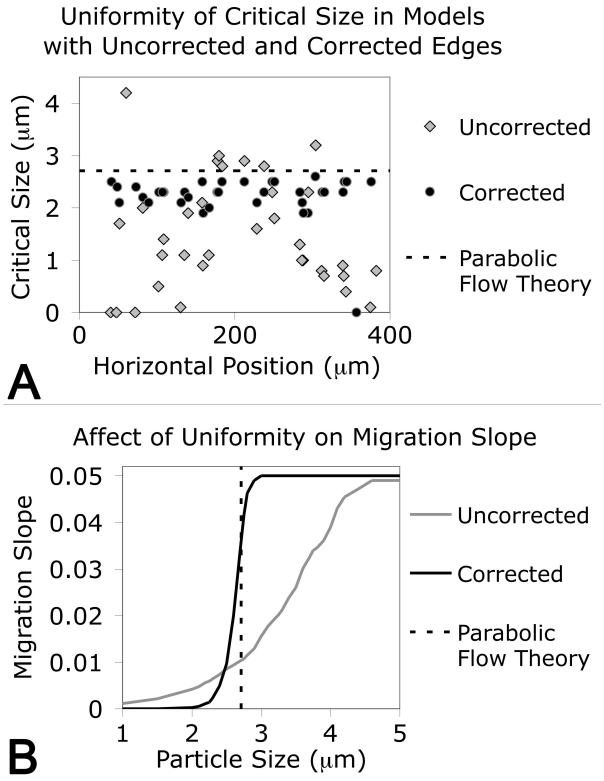

Figure 4: (A) Plot of simulated critical size versus horizontal position for randomly selected positions within the arrays. (B) The poor uniformity in the uncorrected array destroys the characteristic bimodal separation of DLD arrays.

designs shown in Figure 3 by plotting the critical particle size at randomly chosen locations throughout the array. Figure 4A shows the uniformity of the critical size for the two models versus horizontal position. The critical size is assumed to be twice the width of the first streamline, which is determined by tracing stall-lines in the solved model.

This simulation data indicates that for this relatively narrow array prior to correction, the critical particle size in the middle of the array is affected by the boundaries. Moreover correcting the flow at the boundaries has lead to a more uniform critical size throughout (notice the tight grouping of black points in Fig. 4A) and a sharper, more bi-modal separation (Fig. 4B). The effect of variation in critical size is qualitatively similar to the effect caused by particle size dispersion [6].

The migration angle, or slope, is calculated by tracing an imaginary particle through an array having a distribution of critical sizes. The distribution is based on the mean and standard deviation found in Figure 4A. If a particle is above the critical size, it is moved over by the row shift (1.5 μm) and down by the array period (30 μm). If a particle is below the critical size it does not move laterally but does move down by the array period divided by ϵ ($30 \times 20 = 600$ μm). This is repeated 1000 times and the net displacement converted to a migration slope.

The above design was used to build the device shown in Figure 2B. Both devices were designed using L-Edit (Tanner EDA), and patterned using standard photolithography. The master molds were either created directly in SU-8 (Gersteltec, Switzerland) or etched into silicon using a Bosch^{TM} process (Cornell NanoScale Science and Technology Facility) to a depth of about 45 μm. PDMS (polydimethylsiloxane) (GE Silicones RTV615) replicas were made and sealed to glass slides. Images were taken using a inverted epifluorescence microscope and a CCD camera, then processed in ImageJ and Adobe Photoshop. The improvement in Figure 2B is clear as 8.4-μm beads (Bangs) (45% above the critical size) bump as expected from wall to wall, completely depleting at the left boundary and concentrating into a single column at the right boundary.

In summary, we presented a deterministic lateral displacement array of finite width that behaves as an array of infinite width, allowing for efficient concentration of microparticles The array has been developed by designing the interface between the array and the array edge. We have shown with both experiments and simulations that the solution improves performance in the unit cells near the boundary, while in narrow devices the entire array is improved.

The author is grateful for helpful discussions with Kevin Loutherback and Professors James Sturm and Robert Austin. This work was supported by grants from the Australian Research Council (DP0880205) and the Fluorescence Applications in Biotechnology and Life Sciences network.

References

[1] L. R. Huang and E. C. Cox and R. H. Austin and J. C. Sturm, "Continuous particle separation through deterministic lateral displacement," *Science*, vol. 304, pp. 987–990, May 2004.

[2] D. W. Inglis and J. A. Davis and R. H. Austin and J. C. Sturm, "Critical particle size for fractionation by deterministic lateral displacement," *Lab Chip*, vol. 6, pp. 655–658, 2006.

[3] J. A. Davis, D. W. Inglis, K. M. Morton, D. A. Lawrence, L. R. Huang, S. Y. Chou, J. C. Sturm and R. H. Austin, "Deterministic hydrodynamics: taking blood apart," *Proc. Nat. Acad. Sci. (USA)*, vol. 103, pp. 14779–14784, 2006.

[4] K. J. Morton, K. Loutherback, D. W. Inglis, O. K. Tsui, J. C. Sturm, S. C. Chou and R. H. Austin, "Crossing microfluidic streamlines to lyse, label and wash cells," *Lab Chip*, vol. 8, pp. 1448–1453, 2008.

[5] K. J. Morton, K. Loutherback, D. W. Inglis, O. K. Tsui, J. C. Sturm, S. C. Chou and R. H. Austin, "Hydrodynamic metamaterials: Microfabricated arrays to steer, refract, and focus streams of biomaterials," *Proc. Nat. Acad. Sci. (USA)*, vol. 105, pp. 7434–7438, 2008.

[6] M. Heller and H. Bruus, "A theoretical analysis of the resolution due to diffusion and size-dispersion of particles in deterministic lateral displacement devices," *J. Micromech. Microeng.*, vol. 18, pp. 075030, 2008.